Multi-Frequency VLBI Observations of GHz-Peaked Spectrum Sources

S. Kameno[1], M. Inoue[1], Z.-Q. Shen[2], S. Sawada-Satoh[3], and K. Wajima[4]

[1] National Astronomical Observatory of Japan, 2-21-1 Osawa, Mitaka, Tokyo 181-8588 Japan
[2] Shanghai Astronomical Observatory, 80 Nandan Road, Shanghai 200030, China
[3] Academia Sinica Institute of Astronomy and Astrophysics, P.O. Box 23-141, Taipei 106, Taiwan
[4] Korea Astronomy Observatory, 61-1 Hwaam-dong, Yuseong, Daejeon 305-348, Korea

Abstract. We report results of pentachromatic VLBI survey for 18 GHz-peaked spectrum sources. Spectral fitting at every pixel across five frequencies allows us to illustrate distribution of optical depth in terms of free–free absorption or synchrotron self absorption. Quasars and Seyfert 1 sources show one-sided morphology with a core at the end where the optical depth peaks. Radio galaxies and Seyfert 2 show symmetric double-sided jets with a optically thick core at the center.

1. Introduction

GHz-Peaked Spectrum (GPS) sources are powerful radio sources associated with active galactic nuclei, which show a convex radio spectrum peaked at GHz frequencies and a compact overall size smaller than kpc dimension (O'Dea, Baum, & Stanghellini 1991; O'Dea 1998).

A power-law spectrum at frequencies higher than the spectral peak is produced by optically thin synchrotron radiation. A spectral cutoff indicates that the synchrotron emission is optically thick at lower frequencies than the peak, in terms of synchrotron self absorption (SSA) or free–free absorption (FFA).

O'Dea & Baum (1997) and Snellen et al. (2000) showed correlation between the peak frequency and the overall linear size, and claimed that SSA controls the the peak frequency. On the other hand, Bicknell, Dopita, & O'Dea (1997) pointed out that FFA through ionized gas surrounding radio lobes can also produce the correlation between the peak frequency and the overall size. Evidence for FFA was found via multi-frequency VLBI observations in particular GPS sources (e.g. NGC 1052; Kameno et al. 2001; Vermeulen et al. 2003; Kameno et al. 2003; Kadler et al. 2004).

A power-law spectrum of synchrotron emitter through FFA will be affected as

$$S_\nu = S_0 \nu^\alpha \exp(-\tau_0 \nu^{-2.1}), \tag{1}$$

where τ_0 is the optical depth at 1 GHz. τ_0 is related with the electron density n_e and temperature T_e as $\tau_0 = \int_{LOS} 0.46 n_e^2 T_e^{-3/2} dL$. Thus, multi-frequency VLBI observations enable spectral fitting at every pixel to measure τ_0 and illustrate the distribution of cold dense plasma.

2. The Survey

We have carried out five-frequency VLBI observations for 18 GPS sources. The VSOP was used at 1.6 and 4.8 GHz to obtain comparable beam sizes with those at 2.3, 8.4, and 15.4 GHz with the VLBA.
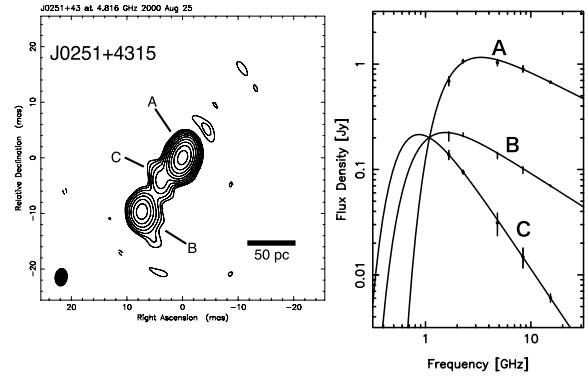
Fig. 1. Morphology and spectra of a type-1 GPS source J0251+4315 .
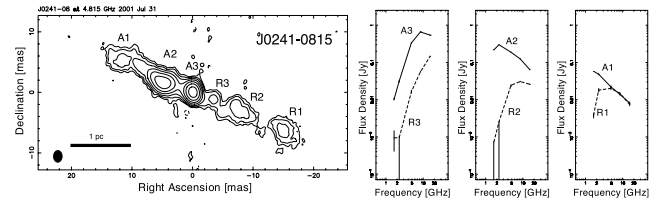
Fig. 2. Morphology and spectra of a type-2 GPS source J0241−0815.

Detailed image performance is shown in the URL `http://vsop.mtk.nao.ac.jp/%7Ekameno/GPSsurvey/`.

Table 1 lists the sample sources which were selected from the GPS catalog by de Vries, Barthel, & O'Dea (1997). Selection criteria of (1) peak frequency ν_m stand within 1.6 GHz < ν_m < 15 GHz, (2) flux density limitation of $S_{1.6GHz}$ > 0.1 Jy, S_{5GHz} > 0.5 Jy, and S_{15GHz} > 0.2 Jy, are applied. Five radio galaxies and 13 quasars are included in the sample.

Images at five frequencies are restored with a common Gaussian beam whose FWHM is a geometric mean of five synthesized beams. These images are registered by referencing several distinct components. Then, spectral fitting was applied for every pixel across five frequencies using equation 1.

Table 1. GPS sample sources.

J2000	other	z	class	α
J0111+3906	0108+388	0.66847	2	−1.1
J0203+1134	0201+113	3.6109	1	−0.3
J0241−0815	NGC 1052	0.0049	2	−1.0
J0251+4315	0248+430	1.31	1	−1.0
J0503+0203	0500+019	0.58457	2	−1.0
J0650+6001	0646+600	0.455	1	−0.6
J0741+3112	0738+313	0.635	1	−0.5
J0745+1011	0742+103	–	1	−0.7
J0745-0044	0743-006	0.994	1	−1.0
J0905+4850	0902+490	2.690	1	−0.7
J1146-2447	1143-245	–	1	−0.7
J1335+4542	1333+459	2.449	1	−1.2
J1845+3541	1843+356	0.746	2	−1.0
J1850+2825	1848+283	2.56	1	−0.7
J2052+3635	2050+364	0.354	2	−1.5
J2129-1538	2126-158	3.268	1	−0.7
J2151+0552	2149+056	0.74	1	−0.75
J2340+2641	2337+264	–	1	−0.7

Columns: (1) IAU source name; (2) other source name; (3) redshift; (4) classification. type-1 stands for quasars and Seyfert 1, where type-2 for radio galaxies and Seyfert 2; (5) spectral index at frequencies above the peak.

Figure 1 and 2 show total intensity maps and results of spectral fit for archetypes of type-1 (J0251+4315) and -2 (J0241−0815). Figure 3 shows profiles of τ_0 along the jet.

Most of type-1 sources (J0203+1134, J0251+4315, J0650+6001, J0741+3112, J0745-0044, J0905+4850, J1146-2447, J1335+4542, J2129-1538, J2151+0552, J2340+2641) show core-jet structure, though J0745+1011 and J1850+2825 are almost unresolved. The optical depth tends to peak at the core component, which is unresolved and brightest at 15.4 GHz. It decreases downstream along the jet, and enhances at knots or hot spots. This behavior can be understood in the context of synchrotron self absorption.

Opacity profiles in type-2 sources tends to be symmetry along the jets. The optical depth peaks at the central component where the nucleus is considered to be, and decreases both downstream. Spiky profiles at the central component of J0111+3906 and J0241−0815 mark the maximum optical depth of $\tau_0 > 100$, which requires $n_e^2 L > 10^8$ cm^{-6} pc. This profile and extreme column density can be understood by an edge-on plasma torus perpendicular to the jet. J0503+0203 and J1845+3541 shows relatively asymmetric opacity profiles with lower maximum. Slant non-edge-on viewing angle can produce such asymmetry. J2052+3635, the largest object in our sample, show a double lobe with multiple hot spots. A central component, which is slightly visible at only 4.8 GHz, is too weak to measure the optical depth.

3. Conclusions

We have performed pentachromatic VLBI survey for type-1 and -2 GPS sources to illustrate distribution of optical depth. Type-1 sources, consisting of quasars and Seyfert 1, show one-sided core-jet structure. The optical depth peaks at the core
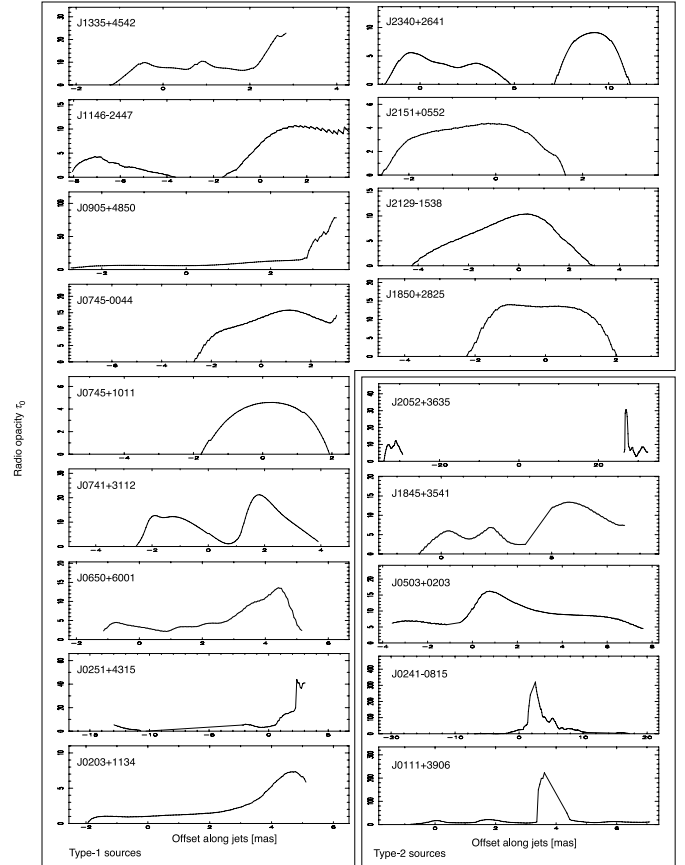
Fig. 3. Opacity profile along jets in GPS sources.

component, and decreases downstream with enhancements at knots and hot spots. Type-2 sources, including radio galaxies and Seyfert 2, show symmetric double-sided structure. The optical depth peaks at the central component with a significantly large opacity.

References

Bicknell, G. V., Dopita, M. A., & O'Dea, C. P. O. 1997, ApJ, 485, 112
de Vries, W. H., Barthel, P. D., & O'Dea, C. P. 1997, A&A, 321, 105
Kadler, M., Ros, E., Lobanov, A. P., Falcke, H., & Zensus, J. A. 2004, *to appear in* A&A
Kameno, S., Inoue, M., Wajima, K., Sawada-Satoh, S., & Shen, Z. 2003, Publications of the Astronomical Society of Australia, 20, 134
Kameno, S., Sawada-Satoh, S., Inoue, M., Shen, Z., & Wajima, K. 2001, PASJ, 53, 169
O'Dea, C. P. & Baum, S. A. 1997, AJ, 113, 148
O'Dea, C. P. 1998, PASP, 110, 493
O'Dea, C. P., Baum, S. A., & Stanghellini, C. 1991, ApJ, 380, 66
Snellen, I. A. G., Schilizzi, R. T., Miley, G. K., de Bruyn, A. G., Bremer, M. N., & Röttgering, H. J. A. 2000, MNRAS, 319, 445
Vermeulen, R. C., Ros, E., Kellermann, K. I., Cohen, M. H., Zensus, J. A., & van Langevelde, H. J. 2003, A&A, 401, 113